Thin-film nucleation through molecular cluster beam deposition: Comparison of tight-binding and many-body empirical potential molecular dynamics simulations

Yanhong Hu
Department of Materials Science and Engineering, University of Florida, Gainesville, Florida 32611

Sanguo Shen, Lei Liu, Chakram S. Jayanthi, and Shi-Yu Wu[a)]
Department of Physics, University of Louisville, Louisville, Kentucky 40292

Susan B. Sinnott[b)]
Department of Materials Science and Engineering, University of Florida, Gainesville, Florida 32611

(Received 4 September 2001; accepted 29 January 2002)

Molecular dynamics simulations are performed to investigate the chemical products of molecular ethylene-cluster beam deposition on diamond substrates at room temperature. The substrates are hydrogen-terminated diamond (111) surfaces of varying sizes. The computational approach is molecular dynamics simulations with two different methods for determining the forces on the atoms: an empirical reactive empirical bond-order hydrocarbon potential and an order-N nonorthogonal tight-binding method. The results of these two approaches to thin-film nucleation through ethylene-cluster beam deposition are compared and contrasted. The results are used to determine the similarities, differences, advantages, and limitations of these two approaches. [DOI: 10.1063/1.1462609]

I. INTRODUCTION

The controlled deposition of hydrocarbon thin films has been achieved by several techniques, including mass selected ion beam deposition,[1–4] chemical vapor deposition,[5,6] and cluster-beam deposition.[7–9] These studies have increased our understanding of the way in which changes in the deposition method, starting material, and reaction conditions influence the results. However, the atomistic mechanisms by which the final product is produced are not available from the experimental data. Therefore, atomistic simulations are used to better understand the fundamental physical and chemical processes that lead to thin-film formation using these methods.[10–12]

Over the last few years Sinnott and co-workers have used classical molecular dynamics (MD) simulations to study hydrocarbon thin-film nucleation on diamond substrates through molecular cluster and cluster-beam deposition. This previous work has shown how cluster molecular species,[13,14] incident kinetic energy,[13–15] cluster size,[16] beam type,[17] surface reactivity,[18] and substrate temperature[17] influence the growth and structure of the resultant thin films. The potentials used in these studies are the reactive empirical bond-order method developed by Brenner[19] for short-ranged covalent interactions coupled to Lennard-Jones potentials[20] for the long-range interactions. While this potential has been shown to be quite good at characterizing reactive processes involving thousands of atoms,[21–25] it is not able to describe processes that depend on the explicit and self-consistent inclusion of electrons.[26]

In this study, MD simulations of molecular cluster deposition on diamond are performed using the reactive empirical bond-order potential of Brenner (EMD) and the order-N nonorthogonal tight-binding MD [O(N)/NOTB-MD] method of Jayanthi, Wu, *et al.*[27] using the NOTB Hamiltonian for carbon developed by Menon *et al.*[28] Tight-binding approaches incorporate real electronic structure and bonding, elements that are lacking in the empirical potential. This scheme has been successfully applied to study a wide range of problems associated with nanostructures, including the initial stage of growth of Si/Si(001),[29] carbon nanotubes,[30] and Si nanoclusters.[31]

The motivation for this work is the desire to check the qualitative and quantitative predictions from these two methods by comparing their results, including the amount of film formation (represented by calculating the percentage of cluster adhesion to the underlying substrates) and the final structures of the nucleated thin films.

II. COMPUTATIONAL DETAILS

A. Reactive empirical bond-order (REBO) potential

In the EMD simulations, the reactive empirical bond-order (REBO) potential for hydrocarbons, developed by Tersoff and refined and parametrized by Brenner, is used to calculate the short-ranged interatomic forces.[19] When this short-ranged potential goes to zero, a Lennard-Jones potential is used to model the long-range van der Waals molecular interactions.[20] Therefore, the combined expression for the binding energy (E_b) between atoms i and j can be expressed in the form

[a)]Electronic mail: sywu0001@fellini.physics.louisville.edu
[b)]Electronic mail: sinnott@mse.ufl.edu

$$E_b = \sum_i \sum_{j(>i)} [V_R(r_{ij}) - B_{ij} V_A(r_{ij}) + V_{\mathrm{vdw}}(r_{ij})], \tag{1}$$

where V_R and V_A are pair-additive interactions that model the interatomic repulsive and attractive forces, respectively, while V_{vdw} is the contribution from long-range van der Waals interactions

$$V_R(r) = f_{ij}^c(r)(1 + Q/r) A e^{-\alpha r}, \tag{2}$$

$$V_A(r) = f_{ij}^c(r) \sum_n b_n e^{-\beta_n r}, \tag{3}$$

$$V_{\mathrm{vdw}}(r) = 4\varepsilon \left[\left(\frac{\sigma}{r} \right)^{12} - \left(\frac{\sigma}{r} \right)^{6} \right], \tag{4}$$

where the subscripts i and j refer to the sum in Eq. (1), the subscript n refers to the sum in Eq. (3), and r_{ij} is the scalar distance between atoms i and j. As described elsewhere,[19,32] the Lennard-Jones potential is zero in the region of covalent interaction and only nonzero after the short-ranged, covalent potential has gone to zero. The two are smoothly joined with a cubic spline. The parameters Q, A, α, b, and β are all parameters that are fit to experimental and *ab initio* data for both hydrocarbon molecules and solid-state carbon[19] and are adjusted using a standard fitting routine. The repulsive pair interaction, shown in Eq. (2), goes to infinity as the interatomic distances approach zero, and the attractive term has sufficient flexibility to simultaneously fit the bond properties. The function $f^c(r)$ limits the range of the covalent interactions. For carbon, the value of $f^c(r)$ will be 1 for nearest neighbors and zero for all other interatomic distances.

B_{ij} is a many-body empirical bond-order between atoms i and j. It is written as the sum of terms

$$\overline{B_{ij}} = \tfrac{1}{2}[B_{ij}^{\sigma-\pi} + B_{ji}^{\sigma-\pi}] + B_{ij}^{\pi}. \tag{5}$$

Values for the functions $B_{ij}^{\sigma-\pi}$ and $B_{ji}^{\sigma-\pi}$ depend on the local coordination and bond angles for atoms i and j. The function B_{ij}^{π} is further written as a sum of two terms

$$B_{ij}^{\pi} = \prod_{ij}^{\mathrm{RC}} + B_{ij}^{\mathrm{DH}}. \tag{6}$$

The value of the first term depends on whether a bond between atoms i and j has radical character and is part of a conjugated system. The value of the second term depends on the dihedral angle for carbon–carbon double bonds.

Unlike traditional valence-force field methods, the atomic bonding in the REBO potential is determined strictly from local bonding neighbors and nonlocal conjugations. Thus this potential allows bond formation and breaking to occur, while the many-body bond-order term allows the coordination of the atoms to change.

B. Order-N nonorthogonal tight-binding molecular dynamics [O(N)/NOTB-MD]

An O(N)/NOTB-MD scheme is also used to carry out quantum-mechanics-based simulations.[27] This scheme is designed to circumvent the N^3 scaling of the calculation of the total energy and atomic forces. Within the framework of the NOTB approach, the band structure energy and the electronic contributions to the atomic forces can be determined by

$$E_{\mathrm{BS}} = 2 \sum_{\lambda(\mathrm{occ})} E_\lambda = 2 \sum_{i\alpha,j\beta} \rho_{i\alpha,j\beta} H_{j\beta,i\alpha}, \tag{7}$$

$$\boldsymbol{F}_{i,\mathrm{el}} = -\frac{\partial E_{\mathrm{BS}}}{\partial \boldsymbol{R}_i} = -2 \sum_{\alpha,j\beta} \left\{ \rho_{i\alpha,j\beta} \frac{\partial H_{j\beta,i\alpha}}{\partial \boldsymbol{R}_i} - \tau_{i\alpha,j\beta} \frac{\partial S_{j\beta,i\alpha}}{\partial \boldsymbol{R}_i} \right\}, \tag{8}$$

where $H_{i\alpha,j\beta}$ and $S_{i\alpha,j\beta}$ are the Hamiltonian matrix element and overlap matrix element, respectively. The density matrix ρ and the energy density matrix τ are defined by

$$\rho_{i\alpha,j\beta} = -\frac{1}{\pi} \lim_{\varepsilon \to 0} \int^{E_F} \mathrm{Im}\, G_{i\alpha,j\beta}(E + i\varepsilon) dE, \tag{9}$$

$$\tau_{i\alpha,j\beta} = -\frac{1}{\pi} \lim_{\varepsilon \to 0} \int^{E_F} E\, \mathrm{Im}\, G_{i\alpha,j\beta}(E + i\varepsilon) dE. \tag{10}$$

Using the property that $\rho_{i\alpha,j\beta}(R_{ij}) \to 0$ and $\tau_{i\alpha,j\beta}(R_{ij}) \to 0$ as $R_{ij} \to \infty$, the summations in Eqs. (7) and (8) can be truncated to include only terms within a sphere of radius R_{cut} if it can be established that $\rho_{i\alpha,j\beta}(R_{ij}) \approx 0$ and $\tau_{i\alpha,j\beta}(R_{ij}) \approx 0$ for $R_{ij} > R_{\mathrm{cut}}$. With the truncation, the calculation of the total energy and the atomic forces will depend linearly on the size of the system. NOTB parameters characterizing the C–H interactions are fit so that the predicted bond lengths and bond angles for C_2H_2, CH_4, C_2H_4, and C_2H_6 are in good agreement with experimental results.

C. Simulation details

The cluster beam investigated in this study contains two molecular ethylene clusters. Each cluster is formed by arranging eight ethylene molecules on a three-dimensional grid in which three-dimensional periodic boundary conditions are applied. Therefore, there are 48 atoms per cluster and 16 of them are carbon atoms. First, the cluster molecules are equilibrated at 500 K. When the cluster has fully relaxed, it is quenched to 5 K to minimize the internal cluster kinetic energy. The cluster is then replicated to form a beam that consists of two clusters with a total diameter of about 8 Å. Before deposition, the whole beam is placed about 4 Å above the surface. The two clusters are then deposited on the surface at an incident energy of 25 eV/molecule, which corresponds to a velocity of 13.1 km/s. The distance between the two clusters in the beam is about 4 Å in the direction normal to the underlying surface. Therefore, the two clusters impact the substrate in a consecutive manner, with the second cluster hitting the surface 30.5 fs after the first.

According to a previous study by the Sinnott group with the REBO potential, different time lags between consecutive cluster deposition results in similar thin-film structures.[15] However, more substrate atoms become part of the thin film when the time lags are small, while more atoms from the

TABLE I. Details of the hydrogen-terminated diamond (111) surfaces used in the study.

Number of atoms in the surface	1260	2352	3136	4480	5824	7168	9216	16 128
Impact area (Å^2)	455.8	615.1	1166.2	1166.2	1166.2	1166.2	1509.3	2672.9
Thickness (Å)	13.0	13.0	13.0	19.1	25.3	31.5	31.5	31.5

cluster remain as part of a thin film when the time lag is long.[15] In this study a short time lag is used because of the emphasis on comparing the results of the O(N)/NOTB-MD and EMD approaches and to minimize the computational costs from the large number of trajectories.

Eight hydrogen-terminated diamond (111) substrates of various sizes are used in this study, and the substrate sizes are given in Table I. The largest substrate contains over ten times as many atoms as the smallest one. These various substrates are chosen in order to compare the computational capability of the two different methods. The EMD method is able to model much larger system sizes than the O(N)/NOTB-MD method. Therefore, a range of system sizes is considered by both methods to determine how the results vary with system size. Prior to cluster deposition, all the substrates are equilibrated at 500 K and then cooled to 300 K, which is the temperature that is maintained throughout the deposition process. Periodic boundaries are applied within the surface plane.

In order to mimic the heat dissipation of a real substrate and maintain the system temperature at 300 K during the deposition, a velocity-rescaling thermostat is used in both the EMD and O(N)/NOTB-MD simulations. Approximately 3–5 rows of atoms at the edges and the carbon atoms of the lower half of the whole surface slab have a thermostat applied to them. Therefore, the thermostat atoms form a bathtub-like shape, helping to control the system temperature. The total number of thermostat atoms is 959, 1768, 2307, 3002, 4320, 5134, 6408, and 10 464 for surfaces containing 1260, 2352, 3136, 4480, 5824, 7168, 9216, and 16 128 atoms, respectively. The bottom layer of hydrogen atoms for each surface is held rigid to maintain the substrate structure during deposition. All the other atoms in the substrate and in the cluster beam evolve without any additional constraints.

During deposition, the majority of the incident energy of the cluster molecules is transformed into excess surface kinetic energy. In the case of the larger surfaces considered, this excess surface kinetic energy is quickly dissipated by the thermostat atoms and does not bounce back to interfere with the chemical interactions taking place at the surface. One measure of this rapid dissipation of energy is the surface temperature at the time of the impact of the second cluster which, for the larger surfaces considered, is about 400–500 K. However, in the smaller surfaces this dissipation does not take place quickly enough and the excess energy is reflected back from the bottom of the surface (this occurs whether or not the bottom layer is held rigid). (This is indicated in the surface temperature at the time of the impact of the second cluster that, for the smaller surfaces considered, is about 700–1100 K.) This reflection of energy seems to occur in somewhat different degrees in the EMD and O(N)/NOTB-MD simulations (see the discussion below). As the point of this study is the comparison of the predictions of these two methods, this reflection of energy does not detract from the study's objectives.

For statistical purposes, several trajectories are performed for each surface and the results are averaged. In the case of the O(N)/NOTB-MD simulations, three trajectories are run for each of the three smallest surfaces (1260, 2352, and 3136 atoms/surface). In the case of the EMD simulations, the same three trajectories are run on the same three surfaces so that the EMD and O(N)/NOTB-MD results may be compared. In addition, since the EMD method is much faster than the O(N)/NOTB-MD method and more trajectories lead to better statistical representation of the results, ten trajectories total are also run for each of the eight surfaces considered (shown in Table I).

The time step is 0.2 fs in the deposition simulations and 0.1 fs in calculating the potential energy surfaces. In all cases, the simulations run for at least 1 ps, with the clusters impacting on the surface during the first 0.16 ps and the film relaxing the rest of the time. Each O(N)/NOTB-MD simulation typically required 12 nodes of an IBM RS/6000 SP2 supercomputer (with 48 CPUs) and ran for about 4 days, while each EMD simulation typically ran for a few hours (the largest simulations ran about 1 day) on a Compaq Alpha64 workstation.

III. RESULTS AND DISCUSSION

When the molecular clusters come into contact with the surface, numerous chemical reactions occur among the cluster molecules and between the cluster and the substrate, resulting in hydrocarbon thin-film nucleation and growth. Both the O(N)/NOTB-MD and EMD methods predict that when the clusters impact the substrate with the short time lag of 30.5 fs, many more of the carbon atoms in the film are from the first cluster that is deposited. Furthermore, both methods predict that within a given cluster, more atoms from the lower half of the cluster (closest to the substrate) remain behind to form the film. These results agree with previous simulation results for molecular cluster deposition.[13,15] Previous studies showed that the elastic collisions among the cluster molecules are responsible for the chemical reactions.[13] Deposition of single molecules does not result in appreciable thin-film formation unless done at high fluence in a larger beam than those considered here.[17]

The atoms that are identified as being part of the thin film include substrate atoms that are displaced from their

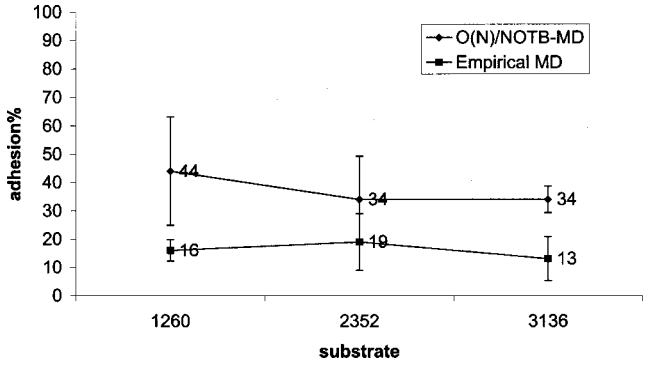

FIG. 1. Percentage of carbon atoms in the incident beam that adhere to the substrates predicted by the O(N)/NOTB-MD and EMD approaches (averaged over three trajectories for surface with 1260, 2352, and 3136 atoms).

original positions and pushed up into the film while still maintaining a connection to the substrate. In addition, some atoms from the cluster penetrate deeply into the substrate beyond the range of the film. Although these atoms are included in the calculation of the number of atoms from the cluster that adhere to the surface, they are not considered when the structure of the film is determined.

The percentage of cluster carbon atoms adhering to the surfaces with 1260, 2352, and 3136 atoms/surface predicted by O(N)/NOTB-MD and EMD is shown in Fig. 1, with detailed numbers provided in Table II. The O(N)/NOTB-MD method predicts a higher percentage of adhesion (approximately 20%–30% more) than the EMD does for the same

TABLE II. The number and percentage of carbon atoms in the incident beam that adhere to the surfaces predicted by the O(N)/NOTB-MD and EMD approaches (averaged over three trajectories).

Number of atoms in the surface	1260	2352	3136
TBMD	14 (44%)	11 (34%)	11 (34%)
Empirical MD	5 (16%)	6 (19%)	4 (13%)

surface in each case. In the EMD case, when the distance between two atoms is less than 1.73, those two atoms are considered to have formed a bond. In the case of the O(N)/NOTB-MD approach, when the number of electrons in the bond region is greater than or equal to 0.04, a bond is considered to be formed.[33] When the distance approach is compared to the electron counting approach for the same set of O(N)/NOTB-MD results, the electron counting approach is found to yield results consistent with those of the distance approach in that there is no bond determined on the basis of the electron counting approach with a bond length greater than 1.73 Å. Hence, the difference in the percentage of adhesion between the two approaches is due to differences inherent to the empirical and tight-binding methods themselves.

To better characterize this difference, the potential energy surfaces of three reactions are considered from static calculations using the REBO and O(N)/NOTB-MD potentials, and the results are plotted in Fig. 2. The first case is the

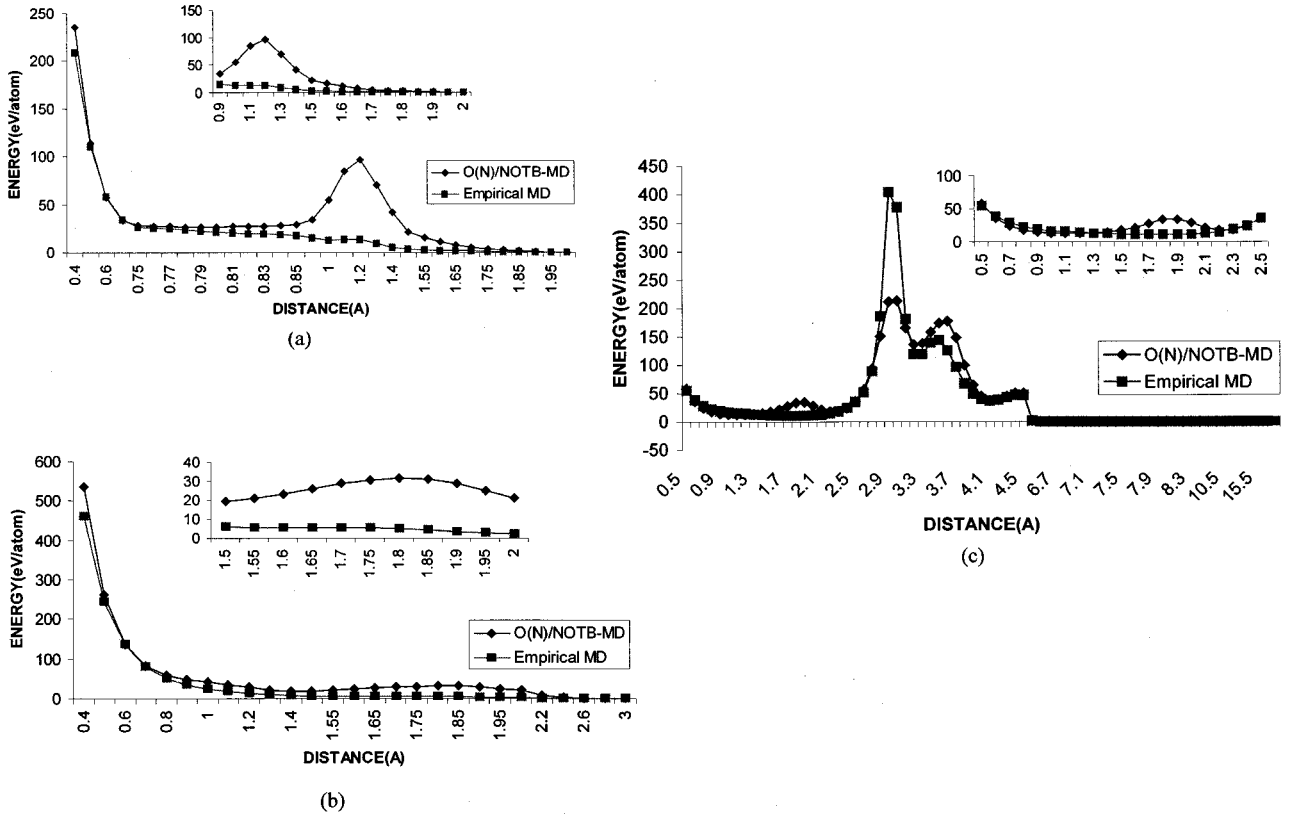

FIG. 2. Comparison of the potential energy surfaces calculated with the tight-binding and empirical potentials for (a) the movement of two ethylene molecules towards each other in a direction horizontal to the double bonds; (b) the movement of two ethylene molecules towards each other in a direction perpendicular to the double bonds; and (c) the movement of two ethylene clusters (each with eight molecules/cluster) towards one another.

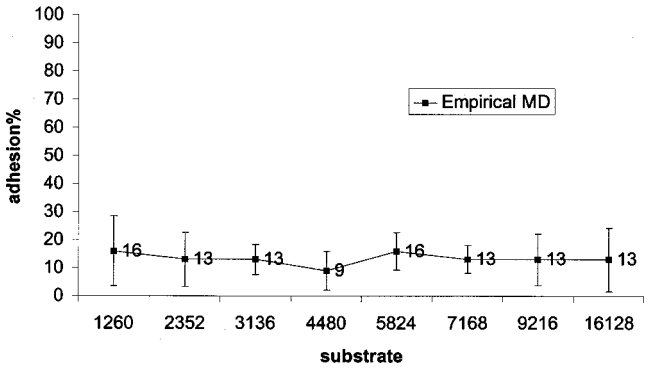

FIG. 3. Percentage of carbon atoms in the incident beam that adhere to the substrates predicted by the EMD approach (averaged over ten trajectories for each surface).

movement of two ethylene molecules towards each other along a path that is horizontal to the double bonds, shown in Fig. 2(a). The second case is the movement of two ethylene molecules towards each other along a path that is perpendicular to the double bonds, shown in Fig. 2(b). Finally, the third case is the movement of two molecular clusters of ethylene (where each cluster contains eight molecules) towards each other, shown in Fig. 2(c).

If one ignores the fine details, one will be struck by the similarities in the overall shapes of the energy curves obtained by the two approaches. This is particularly true in the third case, where the energy curves between two molecular clusters of ethylene obtained by the two methods have remarkably similar shapes. However, there is also a crucial difference between the energy curves obtained by the two methods. From Fig. 2, it can be seen that, in all three cases, there are regions of separation close to the C–C bond length where the energy obtained by the NOTB Hamiltonian is less than that obtained by the REBO potential [see the insert in Fig. 2(c)]. The similarities of the energy curves obtained by the two methods are indications that the REBO potential has indeed captured some general character of carbon-based chemistry. But, the differences show that the REBO potential does not predict the potential barriers to reactions as well as, and is also more rigid than, the NOTB Hamiltonian. It therefore may not be sufficiently flexible to describe all the relevant processes of bond breaking and bond forming in cluster-beam deposition, thus leading to a lower percentage of adhesion for the EMD results. The key is that the NOTB Hamiltonian predicts a more attractive interaction and in general a lower potential barrier in the region of bond breaking and bond formation than the REBO potential.

As the surface size increases, both the O(N)/NOTB-MD and EMD simulations predict that the adhesion percentage is approximately constant. When ten trajectories of EMD simulations are averaged for each of the eight substrates shown in Table I, the results also display little variation in the adhesion percentage with the changing substrate (see Fig. 3 and Table III). This indicates that while the reflection of energy in the case of the smaller surfaces has an effect on the chemical reactions, it is within the error bars that represent the deviation in the averaged results from the multiple trajectories (three trajectories in Fig. 1, ten trajectories in Fig. 3). Other factors that contribute to this deviation include changes in the precise impact sites on the surfaces, thermal fluctuations, and changes in the elastic collisions among the cluster molecules that have been shown to be crucial to the formation of new chemical bonds.[16]

TABLE III. Number and percentage of carbon atoms in the incident beam that adhere to the surfaces predicted by the EMD approach (averaged over ten trajectories).

Number of atoms in the surface	1260	2352	3136	4480	5824	7168	9216	16 128
Number	5	4	4	3	5	4	4	4
Percentage (%)	16	13	13	9	16	13	13	13

Typical snapshots of the nucleated thin films predicted by the O(N)/NOTB-MD and EMD simulations are given in Figs. 4(a) and 4(b), respectively. It is clear that the absorbed species are denser and spread more widely in the O(N)/NOTB-MD simulations, while in the EMD simulations they are more chain-like. These comparisons are made in a more quantitative manner by determining the hybridization of the carbon atoms in the film and the manner in which the carbon atoms are bonded to the other carbon atoms in the film (hereafter referred to as carbon connectivity).

Table IV summarizes the coordination of the carbon atoms in the films predicted to form in the O(N)/NOTB-MD and EMD simulations for surfaces with 1260, 2352, and 3136 atoms/surface. Compared to the EMD results, the O(N)/NOTB-MD method predicts the formation of a higher percentage of sp^3-hybridized carbon, less sp^2-hybridized, and no sp-hybridized carbon. In the EMD simulations, the hybridization of the carbon in the film ranges from sp to sp^3. In other words, the O(N)/NOTB-MD simulations predict the formation of a highly saturated thin-film structure while the EMD simulations predict the formation of a more unsaturated structure. Table V summarizes the averaged hybridization of the carbon atoms in the films formed on all eight surfaces (averaged over ten trajectories).

A close examination of Tables IV and V reveals a role reversal in the percentages of carbon atoms with sp^2 and sp^3

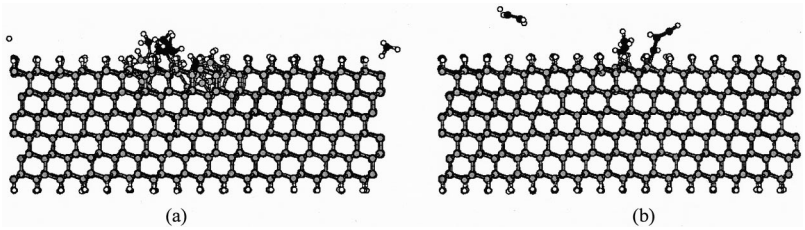

FIG. 4. Snapshots of the nucleated thin film on a hydrogen-terminated diamond (111) surface containing 3136 atoms. The black spheres are the carbon atoms in the cluster beam, the gray spheres are the substrate carbon atoms, and the white spheres are hydrogen atoms. (a) O(N)/NOTB-MD result; (b) EMD result.

TABLE IV. The hybridization of the carbon atoms in the film predicted by the O(N)/NOTB-MD and EMD simulations (averaged over three trajectories) (%).

Number of atoms in the surface		1260	2352	3136
TBMD	sp	⋯	⋯	⋯
	sp^2	22	16	13
	sp^3	78	84	87
Empirical MD	sp	8	12	8
	sp^2	23	65	64
	sp^3	79	23	28

TABLE VI. The carbon connectivity of the carbon atoms in the film predicted by O(N)-NOTB-MD and EMD simulations (averaged over three trajectories) (%).

Number of atoms in the surface		1260	2352	3136
TBMD	C1	30	29	42
	C2	46	37	29
	C3	22	34	25
	C4	2	⋯	4
Empirical MD	C1	49	30	46
	C2	37	65	54
	C3	14	5	⋯

bonding in the film between the 1260 and 2352 atoms/surface cases for the EMD simulations while no such reversal is seen for the O(N)/NOTB-MD simulations. This observation can be understood as follows. For EMD simulations, the 1260-atom surface is just too small to allow for a quick dissipation of any substantial amount of the excess surface kinetic energy. Furthermore, the smallness of the surface slab allows for the reflected excess energy to quickly break up the remnant sp^2-bonded structures in the incoming clusters. This action, in turn, promotes more chemical reactions at the surface, leading to a larger percentage of sp^3-bonded carbon atoms. The 2352-atom surface, on the other hand, is large enough to dissipate some of the excess energy such that the reflected energy is not sufficient to break up the remnant stable sp^2-bonded structures in the incoming clusters, but is still enough to break up some of the newly formed sp^3-bonded structures at the surface. This facilitates the formation of additional sp^2-bonded structures. As the size of the surface increases further, the effect of the reflected energy decreases more. This trend can be clearly seen from the results shown in Table V.

For the O(N)/NOTB-MD simulations, because the NOTB Hamiltonian is more flexible, the excess surface kinetic energy dissipates more quickly than the corresponding situation in the EMD simulations. Hence, even for the 1260-atom surface, some of the excess energy has already been dissipated to the extent that the reflected energy is only sufficient to break up the sp^3 structures formed as a result of chemical reactions at the surface. The effect of the reflected energy is reduced as the surface size increases, as seen in Table IV. The results in Tables IV and V also seem to suggest that the effect of the reflected energy has almost disappeared for the 7168-atom surface in the case of EMD simulations and for the 3136-atom surface in the case of O(N)/NOTB-MD simulations. Finally, the differences in the distribution of the percentages of sp^2- and sp^3-bonded structures between the two cases can be attributed to the rigidity of the REBO potential vs the flexibility of the NOTB Hamiltonian.

The carbon connectivity within the nucleated films predicted by the O(N)/NOTB-MD and EMD simulations for surfaces with 1260, 2352, and 3136 atoms/surface are shown in Table VI. In the table, C1 stands for the percentage of carbon atoms connected to one other carbon atom, C2 stands for the percentage of carbon atoms connected to two other carbon atoms, etc. Therefore, the summation of C1 and C2 indicates the percentage of carbon atoms in a linear structure in the thin film while C3 and C4 indicate the percentage of carbon atoms in branched and networked structures, respectively. It should be pointed out that the hybridization of a carbon atom includes its bonds to both carbon and hydrogen. In contrast, carbon connectivity includes only bonds to other carbon atoms. But, of course, there are some relationships between the two. For example, those carbon atoms that are labeled C4 must be sp^3 hybridized, but sp^3-hybridized carbon atoms do not correlate exclusively with C4 carbons.

For each surface, the carbon connectivity within the film predicted by O(N)/NOTB-MD is different from what is predicted by the EMD simulations. In general, O(N)/NOTB-MD predicts more branched or networked structures and less linear structure than the EMD simulations do. When both the coordination and the carbon connectivity of the film carbon atoms are considered, the O(N)/NOTB-MD method is found to predict the formation of a more diamond-like thin film while the EMD simulations predict a more polymer-like thin film (see Table VII).

IV. CONCLUSIONS

The simulation results for ethylene molecular cluster deposition predicted by O(N)/NOTB-MD and EMD simulations are compared. The results of these two methods do not

TABLE V. The hybridization of the carbon atoms in the film predicted by the EMD simulations (averaged over ten trajectories) (%).

Number of atoms in the surface	1260	2352	3136	4480	5824	7168	9216	16128
sp	17	12	7	3	20	20	15	11
sp^2	29	58	53	70	53	45	46	44
sp^3	54	30	40	27	27	35	39	45

TABLE VII. Carbon connectivity of the carbon atoms in the film predicted by EMD simulations (averaged over ten trajectories) (%).

Number of atoms in the surface	1260	2352	3136	4480	5824	7168	9216	16 128
C1	40	32	47	41	45	39	38	42
C2	54	65	50	50	53	56	54	53
C3	6	3	3	9	2	5	8	5

agree perfectly with each other. For instance, the structures of the resultant thin film are significantly different from one another. Nevertheless, both methods predict thin-film nucleation. We have identified the reason for the difference in the thin-film structure predicted by the two methods as due to the inherent difference between the REBO potential and the NOTB Hamiltonian, namely, the rigidity of the REBO potential vs the flexibility of the NOTB Hamiltonian.

Although O(N)/NOTB-MD is the more accurate method, it is more computationally expensive than the EMD method for a surface of a given size. However, we have also found evidence that it only requires reasonably small surface slabs to eliminate the effect of reflected energy for the O(N)/NOTB-MD simulations. Thus, it is likely that O(N)/NOTB-MD simulations can be applied to study systems considered in this work and similar systems if more trajectories are included to improve the statistics.

ACKNOWLEDGMENTS

The authors thank Thomas Plaisted and Donald Brenner for many useful discussions. S.B.S. acknowledges the support of the NSF through Grant No. (CHE-9708049), while C.S.J and S.Y.W. acknowledge the support of the DOE through Grant No. (DE-FG02-OOER45832) and the NSF through Grant No. (DMR-9802274).

[1] M. B. J. Wijesundara, L. Hanley, B. Ni, and S. B. Sinnott, Proc. Natl. Acad. Sci. U.S.A. **97**, 23 (2000).
[2] M. B. J. Wijesundara, Y. Ji, B. Ni, S. B. Sinnott, and L. Hanley, J. Appl. Phys. **88**, 5004 (2000).
[3] E. T. Ada, O. Kornienko, and L. Hanley, J. Phys. Chem. B **102**, 3959 (1998).
[4] W. M. Lau and R. W. M. Kwok, Int. J. Mass Spectrom. Ion Processes **174**, 245 (1998).
[5] J. C. Angus and C. C. Hayman, Science **241**, 913 (1988).
[6] K. E. Spear, J. Am. Ceram. Soc. **72**, 171 (1989).
[7] L. Diederich, E. Barborini, P. Piseri, A. Podesta, P. Milani, A. Chneuwly, and R. Gallay, Appl. Phys. Lett. **75**, 2662 (1999).
[8] V. Paillard, P. Melinon, V. Dupuis, A. Perez, J. P. Perez, G. Guiraud, J. Fornazero, and G. Panczer, Phys. Rev. B **49**, 11433 (1994).
[9] E. E. B. Campbell and I. V. Hertel, Nucl. Instrum. Methods Phys. Res. B **112**, 48 (1996).
[10] W. Christen and U. Even, J. Phys. Chem. A **102**, 9420 (1998).
[11] D. Donadio, L. Colombo, P. Milani, and G. Benedek, Phys. Rev. Lett. **83**, 776 (1999).
[12] M. Kerford and R. P. Webb, Carbon **37**, 85 (1999).
[13] L. Qi and S. B. Sinnott, J. Phys. Chem. B **101**, 6883 (1997).
[14] L. Qi and S. B. Sinnott, J. Vac. Sci. Technol. A **16**, 1293 (1998).
[15] L. Qi and S. B. Sinnott, Surf. Sci. **398**, 195 (1998).
[16] L. Qi and S. B. Sinnott, Nucl. Instrum. Methods Phys. Res. B **140**, 39 (1998).
[17] T. A. Plaisted, B. Ni, J. D. Zahrt, and S. B. Sinnott, Thin Solid Films **381**, 73 (2001).
[18] L. Qi, W. L. Young, and S. B. Sinnott, Surf. Sci. **426**, 83 (1999).
[19] D. W. Brenner, Phys. Status Solidi B **217**, 23 (2000).
[20] Z. Mao, A. Garg, and S. B. Sinnott, Nanotechnology **10**, 273 (1999).
[21] E. R. Williams, G. C. Jones, L. Fang, R. N. Zare, B. J. Garrison, and D. W. Brenner, J. Am. Chem. Soc. **114**, 3207 (1992).
[22] D. R. Alfonso, S. E. Ulloa, and D. W. Brenner, Phys. Rev. B **49**, 4948 (1994).
[23] J. N. Glosli and F. H. Ree, J. Chem. Phys. **110**, 441 (1999).
[24] A. V. Petukhov, D. Passerone, F. Ercolessi, E. Tosatti, and A. Fasolino, Phys. Rev. B **61**, R10590 (2000).
[25] S. R. Schofield, M. W. Radny, and P. V. Smith, Phys. Rev. B **62**, 10199 (2000).
[26] P. De Sainte Clare, K. Son, W. L. Hase, and D. W. Brenner, J. Am. Chem. Soc. **100**, 1761 (1996).
[27] C. S. Jayanthi, S. Y. Wu, J. Cocks, N. S. Luo, Z. L. Xie, M. Menon, and G. Yang, Phys. Rev. B **57**, 3799 (1998).
[28] M. Menon, K. R. Subbaswamy, and M. Sawtarie, Phys. Rev. B **48**, 8398 (1993).
[29] S. Liu, C. S. Jayanthi, S. Y. Wu, X. R. Qin, Z. Zhang, and M. Lagally, Phys. Rev. B **61**, 4421 (2000).
[30] T. W. Tombler, C. Zhou, L. Alexseyev, J. Kong, H. Dai, L. Liu, C. S. Jayanthi, and S. Y. Wu, Nature (London) **405**, 769 (2000).
[31] L. Liu, C. S. Jayanthi, and S. Y. Wu, J. Appl. Phys. **90**, 4143 (2001).
[32] S. B. Sinnott, O. A. Shenderova, C. T. White, and D. W. Brenner, Carbon **36**, 1 (1998).
[33] D. R. Alfonso, S. Y. Wu, C. S. Jayanthi, and E. Kaxiras, Phys. Rev. B **59**, 7745 (1999).